CSMA 2022
15ème Colloque National en Calcul des Structures
16-20 Mai 2022, Presqu'île de Giens (Var)

Computation of eigenvectors in heterogeneous media as updates from homogenized estimates

R. Cottereau, D. Colas, C. Bellis, B. Lombard

Aix Marseille Univ, CNRS, Centrale Marseille, LMA UMR 7031, Marseille, France, cottereau@lma.cnrs-mrs.fr

Résumé — In this talk, we discuss the problem of computing eigenvalues and eigenvectors of a heterogeneous material or domain, and the numerical schemes to approximate them. We propose an improvement over the traditional Rayleigh quotient technique for the update of the eigenvalues, and discuss specifically the initialization of the iterative algorithm. We propose to use the homogenized equation to compute initial estimates and assess numerically the behavior of the algorithm when eigenmodes are actually localized.
Mots clés — Waves in heterogeneous media, Vibrations of heterogeneous materials, Eigenvalue analysis, Homogenization, Anderson Localization.

1 The wave equation in heterogeneous media

1.1 The wave equation

In this paper, we consider a domain $\Omega \in \mathbb{R}^d$, and the wave equation for the pressure field $u(\mathbf{x},t)$, with loading $f(\mathbf{x},t)$ and heterogeneous parameters $\rho(\mathbf{x})$ and $\kappa(\mathbf{x})$:

$$\nabla \cdot (\kappa(\mathbf{x})\nabla u(\mathbf{x},t)) + f(\mathbf{x},t) = \rho(\mathbf{x})\frac{\partial^2}{\partial t^2}u(\mathbf{x},t), \quad \forall \mathbf{x} \in \Omega. \tag{1}$$

Dirichlet boundary conditions $u(\mathbf{x},t) = 0$, for $\mathbf{x} \in \partial\Omega$, are additionally considered along with vanishing initial conditions $u(\mathbf{x},0) = 0$ and $\partial u/\partial t(\mathbf{x},0) = 0$. Typically, the problems of interest in this paper are not periodic. Rather, the bulk modulus $\kappa(\mathbf{x})$ and density $\rho(\mathbf{x})$ are modeled as realizations of (statistically homogeneous) random fields. These random field are parameterized by a first-order marginal density, with averages $\underline{\kappa}$ and $\underline{\rho}$ and variances σ_κ^2 and σ_ρ^2, and a correlation function with correlation length ℓ_c.

When considering a numerical method such a the Finite Element Method, the above partial differential equation translates into the matrix problem :

$$\mathbf{K}\mathbf{u}(t) + \mathbf{M}\frac{\partial^2}{\partial t^2}\mathbf{u}(t) = \mathbf{F}(t), \tag{2}$$

where $\mathbf{K}_{ij} = \int_\Omega \kappa \nabla N_i \cdot \nabla N_j d\mathbf{x}$, $\mathbf{M}_{ij} = \int_\Omega \rho N_i N_j d\mathbf{x}$, $\mathbf{F}_i(t) = \int_\Omega N_i f d\mathbf{x}$ for a given set of base functions $N_i(\mathbf{x})$ enforcing the Dirichlet boundary conditions, associated to a set of degrees of freedom, and the vector $\mathbf{u}(t)$ stores the values of the pressure field $u(\mathbf{x},t)$ at these degrees of freedom.

1.2 Eigenvectors and eigenvalues

The properties of the operator of Eq. (1) imply that there exists a countable basis of eigenvectors $\phi_n(\mathbf{x})$, $n \in \mathbb{N}$, with associated eigenvalues $\mu_n > 0$, solution of

$$\nabla \cdot (\kappa(\mathbf{x})\nabla \phi_n(\mathbf{x})) = \rho(\mathbf{x})\mu_n\phi_n(\mathbf{x}), \quad \forall \mathbf{x} \in \Omega, \tag{3}$$

with Dirichlet boundary conditions. These eigenvectors and eigenvalues are useful, among other things, in vibration analysis to diagonalize Eq. (1). The objective of this paper is to discuss numerical schemes to compute the lower eigenvalues and eigenvectors when the domain is heterogeneous. The corresponding discretized formulation is

$$\mathbf{K}\boldsymbol{\phi}_n = \mu_n \mathbf{M}\boldsymbol{\phi}_n, \tag{4}$$

where the vector $\boldsymbol{\phi}_n$ stores the values of the eigenmode $\phi_n(\mathbf{x})$ at the degrees of freedom. Typically, the modes are normalized with respect to mass $\boldsymbol{\phi}_n^T \mathbf{M} \boldsymbol{\phi}_n = 1$, so that we naturally have $\boldsymbol{\phi}_n^T \mathbf{K} \boldsymbol{\phi}_n = \mu_n$.

Most numerical schemes to estimate the eigenvalues and eigenmodes work at the matrix level, Eq. (4), and "forget" the relation with the underlying partial differential equations, Eq. (3). One objective of the paper is to try and use this relation to improve the efficiency of the approximation scheme.

1.3 Low-frequency homogenization in heterogeneous media

Assuming that the correlation length of the random fields $\kappa(\mathbf{x})$ and $\rho(\mathbf{x})$ verifies $\ell_c \ll L \approx \lambda$, where L is the typical dimension of the domain Ω and λ is the typical wavelength, and that the level of fluctuation of the properties is large (typically $\sigma_\kappa/\underline{\kappa} \approx 1$ and $\sigma_\rho/\underline{\rho} \approx 1$, or more), homogenization results hold. This theory was initially derived in the periodic case [2], and then extended to non-periodic media fluctuating at two scales (see the nice results of [3] in dynamics) and random media [8]. It essentially states that the solution of Eq. (1) can be well approximated (the precise meaning of "well" being left aside here for concision purposes) by the so-called homogenized field $u^*(\mathbf{x},t)$, solution of :

$$\nabla \cdot (\kappa^* \nabla u^*(\mathbf{x},t)) + f(\mathbf{x},t) = \rho^* u^*(\mathbf{x},t), \quad \forall \mathbf{x} \in \Omega, \tag{5}$$

where κ^* and ρ^* are (homogeneous) material parameters obtained using classical corrector equations. The interest of this homogenized problem is that the homogenized parameters are homogeneous, which means that approximations of $u^*(\mathbf{x},t)$ can be obtained on a coarser mesh than $u(\mathbf{x},t)$, and hence for a lower computational cost. Note that the homogenization problem is obtained through asymptotic analysis so that boundaries have to be considered apart, but this issue will disregarded here (see for instance [1]).

Similar results were derived (in [6], see also [9, 7]) for the eigenvalue problem. It can be shown that the first eigenvalue and eigenvectors, in Eq. (3), can be well approximated by $(\mu_n^*, \phi_n^*(\mathbf{x}))$, solution of the homogenized eigenvalue problem :

$$\nabla \cdot (\kappa^* \nabla \phi_n^*(\mathbf{x})) = \rho^* \mu_n^* \phi_n^*(\mathbf{x}), \quad \forall \mathbf{x} \in \Omega, \tag{6}$$

where the κ^* and ρ^* are the same as above. As above, approximations of $(\mu_n^*, \phi_n^*(\mathbf{x}))$ can be obtained more easily than approximations of $(\mu_n, \phi_n(\mathbf{x}))$. Note that the condition that $L \approx \lambda$ implies that the approximation is correct only for the lowest eigenmodes. As will be shown in examples below, after the first very few frequencies, the accuracy of the homogenized modes deteriorates, even though the order of magnitude of the homogenized eigenvalues remains meaningful.

2 Rayleigh quotient iterative algorithm

We describe in this section a classical way to compute solutions of Eq. (4).

2.1 Description of the algorithm

Starting from initial estimates (μ_n^0, ϕ_n^0), typically $(0, \mathbf{r})$, where $\mathbf{r}$ is a random vector with independent entries distributed uniformly in $[0,1]$, the Rayleigh quotient algorithm is based on the following updates for the eigenvectors :

$$\boldsymbol{\phi}_n^{k+1} = \left(\mathbf{K} - \mu_n^k \mathbf{M} \right)^{-1} \mathbf{M} \phi_n^k, \tag{7}$$

and eigenvalues

$$\mu_n^{k+1} = \frac{(\boldsymbol{\phi}_n^{k+1})^T \mathbf{K} \boldsymbol{\phi}_n^{k+1}}{(\boldsymbol{\phi}_n^{k+1})^T \mathbf{M} \boldsymbol{\phi}_n^{k+1}}. \tag{8}$$

This latter equation, namely a Rayleigh quotient, is obviously the reason for the name of the algorithm. For $k \to \infty$, the algorithm converges to the pair (μ_0, ϕ_0), where μ_0 is the smallest eigenvalue (assuming that eigenvalue is simple), for which the eigenvector ϕ_0 is not orthogonal to the initial estimate ϕ_n^0. In practice, this algorithm converges very rapidly (see next section for examples), even when the initial estimates are not very good. Once the first eigen-pair has been obtained, further pairs can be computed using a deflation technique, or updating the eigenvectors of Eq. (7) in the space orthogonal to the modes

that have already been computed. Here, we will use the second approach. Note that when approaching convergence, the matrix becomes badly conditioned, so that the criterion we consider to stop the iterative process is based on an approximation of the condition number of the matrix $\mathbf{K} - \mu_n^k \mathbf{M}$. We specifically use the Matlab function `condest`, based on the 1-norm condition estimator of [4] and a block-oriented generalization described in [5].

2.2 Illustration of the behavior of the algorithm

To illustrate how this algorithm works, we consider two Bernouilli examples, in 1D and 2D. The domains are decomposed into segments (respectively squares) of constant size (side) $h = 1$ m for a total side of $L = 1000$ m in 1D and $L = 100$ m in 2D, and the parameters κ and μ are randomly allocated to each segment (respectively square) by drawing from a Bernouilli distribution with two values (1 and 100 for κ, in kg/m/s^2, and 0.1 and 1 for ρ, in kg/m^3) with uniform probabilities. A sample of $\kappa(\mathbf{x})$ is presented in Figure 1 for each of the 1D and 2D cases. The samples of $\rho(\mathbf{x})$ look qualitatively the same, although the amplitudes are not the same, and $\rho(\mathbf{x})$ and $\kappa(\mathbf{x})$ are independent.

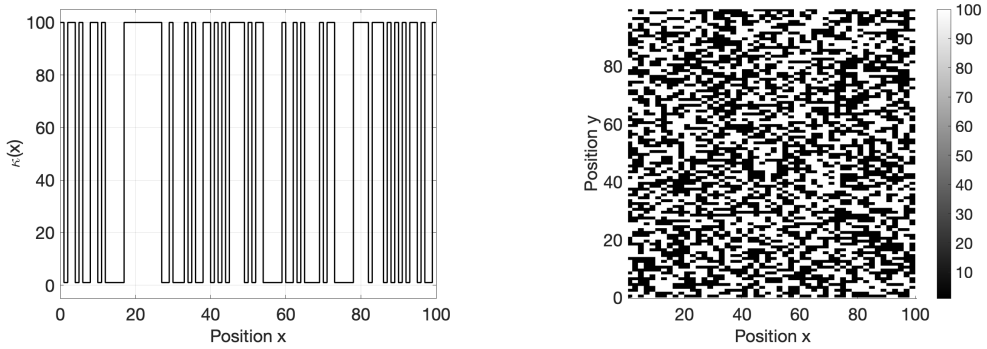

FIGURE 1 – One sample of random field $\kappa(\mathbf{x})$ in 1D (left, restricted to $x = [0, 100]$ m for visibility) and 2D (right).

Figure 2 displays the first eigenvalues and two eigenmodes for the heterogeneous case, as well as for the corresponding homogenized equation, and those arising from the Rayleigh Quotient algorithm, along with the results described in the next section. The eigenmodes obtained by the Rayleigh Quotient have not been plotted here because they overlap exactly the exact modes. Likewise, Figure 2 shows that the eigenvalues that are captured are indeed very well captured. The main issue with the algorithm is therefore that some of the eigenvalues are missing in the sense that the algorithm converges towards another (higher) value than the lowest. The number of iterations is very low (see Figure 4 in next section). The same conclusions can be drawn concerning the 2D example, whose results are displayed on Figures 3 and 5.

3 Improved Rayleigh quotient iterative algorithm

In this section we introduce two improvements with respect to the classical Rayleigh Quotient algorithm.

3.1 Improved evaluation of the eigenvalue

Starting from Eq. (4), we can obtain the following two equivalent definitions of the eigenvalue :

$$\mu_n = \frac{\phi_n^T \mathbf{K} \phi_n}{\phi_n^T \mathbf{M} \phi_n}, \quad \mu_n = \frac{\phi_n^T \mathbf{M} \phi_n}{\phi_n^T \mathbf{M} \mathbf{K}^{-1} \mathbf{M} \phi_n}. \tag{9}$$

The first one is the classical Rayleigh quotient, used in the algorithm above to update the eigenvalue, Eq. (8), but the second can equally well be used for that purpose. This is what we propose as our first improvement. The inconvenient is that it requires to compute the solution of a system at each iteration,

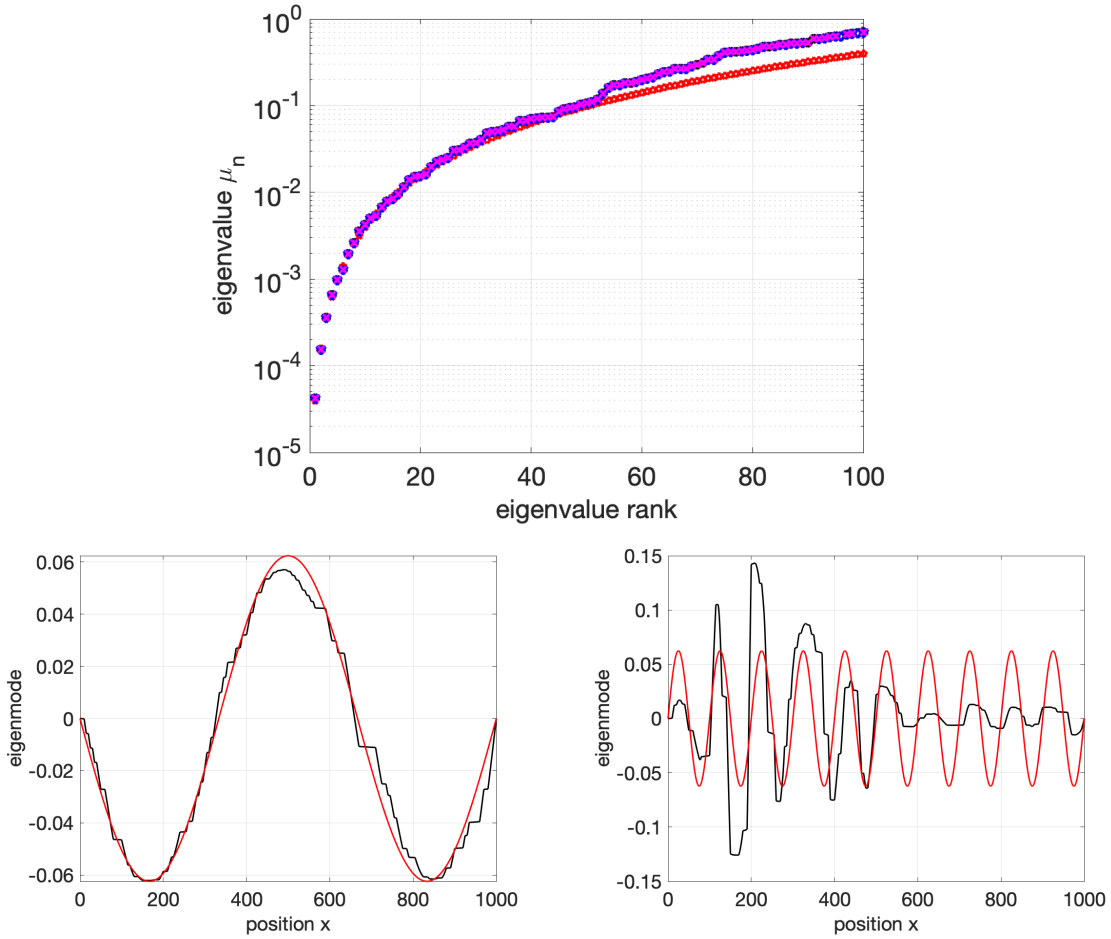

FIGURE 2 – 1D example : first eigenvalues (top) and eigenvectors (3rd mode in the bottom left and 20th on the bottom right) for the heterogeneous (black lines and circles), homogenized (red lines and stars) problems. The eigenvalues obtained using the classical (blue triangles) and improved (magenta crosses) Rayleigh Quotient algorithms are also plotted on the top, and both overlap the exact eigenvalues, although some are missing.

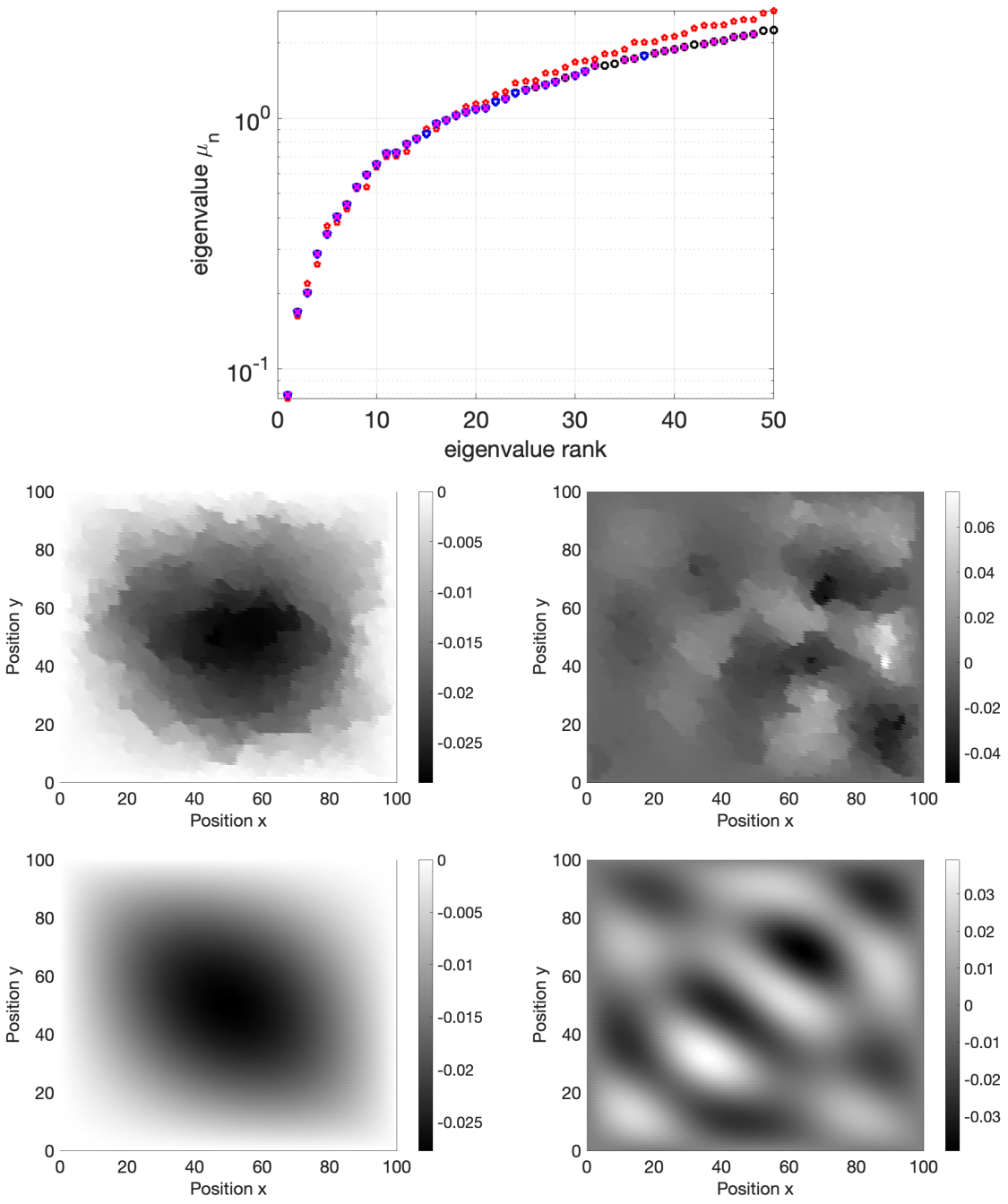

FIGURE 3 – 2D example : first eigenvalues (top) for the heterogeneous (black lines and circles) and homogenized (red lines and stars) models, and eigenvalues estimated by the classical (blue triangles) and improved (magenta crosses) Rayleigh Quotient algorithms. On the left are plotted the first eigenmode of the heterogeneous (center line) and homogenized (lower line) models. On the right are plotted the 20th eigenmode of the heterogeneous (center line) and homogenized (lower line) models.

which induces additional costs. However, we will show in the examples below that it converges slightly better.

Note that this idea came from a trick that we found already in [6] in the context of asymptotic analysis. We have not found further references to it, and believe it is not being used in the context of the Rayleigh Quotient algorithm.

3.2 Initialization with homogenized estimates

The second improvement we propose to use concerns initialization. Observing on Figures 2 and 3 that, at least for the first modes, the homogenized modes are good estimates of the eigenvalues and eigenmodes (see previous section), we propose to use them as initialization for the algorithm. We therefore replace the initialization $(\mu_0^0, \phi_n^0) = (0, \mathbf{r})$ (for the classical Rayleigh Quotient algorithm) by $(\mu_0^0, \phi_n^0) = (\mu_n^*, \phi_n^*)$. It is expected that this choice will haste convergence, even though it requires the solution of the homogenized equation, which is expected to be cheap because the meshing can be coarsened with respect to the heterogeneous case.

3.3 Numerical illustration of the behavior of the improved algorithm

As the Rayleigh Quotient algorithm was shown in the previous section to be working quite nicely, we consider now a more stringent comparison criterion, namely the MAC number, which is a correlation between two eigenmodes. More specifically, a map of MAC numbers can be computed for two sets of eigenmodes, ϕ^1 and ϕ^2 as

$$\mathrm{MAC}_{nm} = \left|(\phi_n^1)^T \mathbf{M} \phi_m^2\right| \tag{10}$$

Such MAC maps are presented for the 1D example in Figure 4 for the modes obtained with the Rayleigh Quotient algorithm (left) on the one hand, and the improved algorithm (center), on the other hand (and on Figure 5 for the 2D example). Each time the set of approximate eigenmodes is compared to the true eigenmodes. The main conclusion is that the modes are well identified in both algorithms, but some modes are missing, as already discussed in the previous section. We also observe that the first missing modes appear earlier with the Rayleigh Quotient algorithm than with our approach, which is a small qualitative advantage of our approach. On Figures 4 and 5 are also plotted distributions of the number of iterations required to converge for each approach in 1D and 2D. These distributions show that our algorithm converges faster, with on average 1 or 2 iterations less.

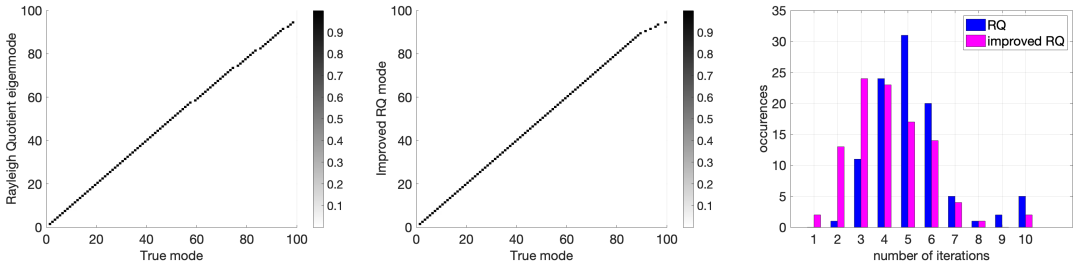

FIGURE 4 – 1D example : MAC numbers between the eigenmodes obtained through the classical Rayleigh Quotient algorithm and the true modes (left) and between those from the improved Rayleigh Quotient algorithm and the true modes (center) ; and distributions of number of iterations for the two algorithms (right).

Note that the algorithm seem to identify less modes than required because we have chosen to show only those that are paired to the 100 modes (in 1D, 50 in 2D). The algorithms actually always converge to a true mode, but this mode may be outside the range that we have decided to show. Note also that additional simulations (not shown here) indicate that the faster convergence is really a consequence of the initialization with homogenized estimates, while the modification of the eigenvalue update leads to missing less eigenvalues.

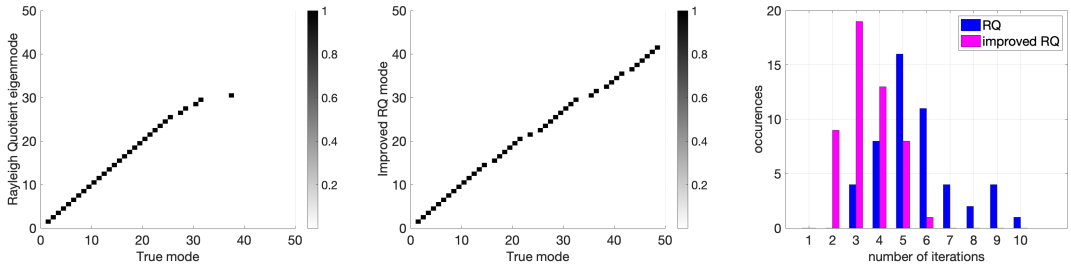

FIGURE 5 – 2D example : MAC numbers between the eigenmodes obtained through the classical Rayleigh Quotient algorithm and the true modes (left) and between those from the improved Rayleigh Quotient algorithm and the true modes (center) ; and distributions of number of iterations for the two algorithms (right).

4 Conclusions

We proposed in this paper two modifications of the classical Rayleigh Quotient algorithm. The first one consists in updating the eigenvalues in a different manner. The cost is the solution of a linear system, and the interest is a slight improvement of the results. Qualitatively, this improvement seems to produce better results in the sense that less eigenvalues are skipped by the algorithm. The second improvement consists in using homogenization to initialize the algorithm. The cost is the solution of a homogenized eigenvalue problem, *a priori* posed for much smaller matrices than the original problem, and with a negligible cost. This initialization leads to a decrease of the number of iterations, even when the actual eigenmode is rather far from the homogenized estimate.

Références

[1] G. Allaire, M. Amar. *Boundary layer tails in periodic homogenization*, ESAIM : Control, Optim. Calc. Variations, 4, 209–243, 1999.

[2] A. Bensoussan, J.-L. Lions, G. Papanicolaou. *Asymptotic analysis for periodic structures*, North Holland, 1978.

[3] Y. Capdeville, J.-J. Marigo. *Second order homogenization of the elastic wave equation for non-periodic layered media*, Geophys. J. Int., 170(2), 823–838, 2007.

[4] W. W. Hager. *Condition estimates*, SIAM J. Sci. Stat. Comput., 5, 311-316, 1984.

[5] N. J. Higham, F. Tisseur. *A Block Algorithm for Matrix 1-Norm Estimation with an Application to 1-Norm Pseudospectra*, SIAM J. Matrix Anal. Appl., 21, 1185-1201, 2000.

[6] S. Kesavan. *Homogenization of elliptic eigenvalue problems : Part 1*, Appl. Math. Optim., 5, 153-167, 1979.

[7] O. A. Oleinik. *On homogenization problems*, Proceedings of the Conference on Trends and Applications of Pure Mathematics to Mechanics, P. G. Ciarlet, M. Roseau (eds), 248–272, 1984.

[8] G. C. Papanicolaou, S. R. S. Varadhan. *Boundary value problems with rapidly oscillating random coefficients*, Proceedings of the Conference on Random Fields, J. Fritz, J. L. Lebowitz (eds), 835–873, 1981.

[9] M. Vanninathan. *Homogenization of eigenvalue problems in perforated domains*, Proc. Indian Acad. Sci. (Math. Sci.), 90(3), 239–271, 1981.